LRP 606/98 October 1998

A MODERN PLASMA CONTROLLER TESTED ON THE TCV TOKAMAK

M. Ariola, G. Ambrosino, J.B. Lister,
A. Pironti, F. Villone, P. Vyas

Submitted for publication to
Fusion Technology

A Modern Plasma Controller Tested on the TCV Tokamak

M. Ariola[1], G. Ambrosino[1], J.B. Lister, A. Pironti[1], F. Villone[2], P. Vyas

Centre de Recherches en Physique des Plasmas
Association EURATOM-Confédération Suisse,
École Polytechnique Fédérale de Lausanne,
CH-1015 Lausanne, Switzerland

[1]Associazione EURATOM-ENEA-CREATE,
Dipartimento di Informatica e Sistemistica,
Università degli Studi di Napoli Federico II
Via Claudio 21, I-80125 Napoli, Italy

[2]Associazione EURATOM-ENEA-CREATE,
Dipartimento di Ingegneria Industriale,
Università di Cassino, I-03043, Cassino (FR), Italy

ABSTRACT

A high order, multivariable, modern plasma controller has been tested on the TCV tokamak. This paper describes an initial design for the control of the plasma current, position and shape parameters. The design process was based on the CREATE-L linearised model of TCV and the controller was implemented on a digital processor. The results demonstrated useful improvements and good agreement with predictions using the model.

1. INTRODUCTION

This paper presents the first results of a modern plasma controller design operating on plasma shape, position and current parameters during a tokamak discharge. We describe the motivation, design and results of this initial experiment on TCV.

Present tokamaks usually use low order controllers that are based on a Proportional-Integral-Derivative (PID) structure. Typically they are partly designed on the basis of simple models of the system to be controlled and are usually fine-tuned during tokamak operation. This combination of techniques has proven to be quite reliable in the past and has usually led to adequate tokamak control performance. The relative simplicity of the models on which the controllers are based can lead to imperfections in the performance, most obvious in the residual coupling between controlled parameters. Such problems only occur during transient events and have been tolerated.

Recently, considerable attention has been focused on the design of plasma position, current and shape controllers for the ITER tokamak. Apart from the pure size of this device, its control has to be relatively stringent with respect to present tokamaks, to avoid wall contact between the hot plasma edge and the walls. The controller is also restricted to demand as little power as possible, to limit surges in the total power required for the Poloidal Field (PF) system. Simulations of the control of the ITER plant by modern controllers have provoked a great deal of interest due to their performance. In particular Linear Quadratic Control, e.g. [1-4], and H_∞ optimal control, e.g. [5-7], have been proposed for tokamak control. These design techniques require an accurate model of the tokamak, which is used in a mathematical optimisation to find a controller minimising a performance cost function. There has been some concern that the rather unpredictable nature of the tokamak, together with noise and internal disturbances, might pose problems for such controllers. The decision was therefore taken to validate the full design procedure of such an advanced controller from both the modelling and controller design aspects. The TCV tokamak possesses a large number of poloidal field coils, all separately powered, and represents a suitable device on which such studies could be performed. Previously, the H_∞ design technique had only been applied on a tokamak for the control of the vertical position on COMPASS-D [8].

The first step required an accurate model of the TCV tokamak. A programme of benchmarking the CREATE-L linearised deformable plasma equilibrium model [9] was undertaken. Closed loop performance comparisons between the modelled tokamak and TCV experiments were carried out for limited discharges [10] and diverted discharges [11] in the presence of external PF coil voltage perturbations. These experiments showed no discrepancies between the model and the experiment. Further closed loop experiments were able to identify the open loop tokamak system, using multiple frequency PF coil voltage stimulation, and there was good agreement between this open loop system identified model and the open loop CREATE-L model [12]. After these three exercises, we considered that we possessed an adequate model of the tokamak. If this were not the case, we doubt that more effort could generate a significantly more accurate model, given all the experimental uncertainties.

Secondly, we had to specify the design goals of the advanced controller, which we shall discuss in some detail in this article.

Thirdly, we had to perform the design of the controller in order to achieve the required performance and test its robustness to noise and variations in the tokamak model.

Fourthly, we had to design and develop a digital plasma control system [13] in which the advanced controller could be implemented.

Finally we had to perform the experiments to confirm that the controller did deliver the proposed performance during typical TCV operation.

In this article, we limit ourselves to the operation of the advanced controller during the "flat top" part of the TCV plasma discharge. A digital implementation of the existing PID controller was used to control the initiation and extinction phases of the

discharge. We were also relatively conservative in this first attempt, restricting ourselves to a mild elongation and therefore a mild vertical instability growth rate.

Careful planning and design of the controller ensured the successful operation of this controller with no extra experimental preparation and no design iterations. This is an important feature of our result.

In the remainder of this paper we present the most relevant properties of the TCV tokamak in Section 2, the specification of the controller design objectives in Section 3, the controller design itself in Section 4, the experimental results in Section 5 and we conclude with a brief discussion in Section 6.

2. TCV TOKAMAK SYSTEMS

A detailed description of the TCV tokamak and its associated control systems can be found in [14]. Figure 1 shows the 18 separate PF coils around a rectangular vacuum vessel. Each PF coil has a separate thyristor power supply driven by a 200MVA motor generator set. In previous work we showed that it was important to model the power supplies correctly and a suitable model using a single pole filter with a time constant of 0.3msec was chosen [10].

The original TCV plasma control system was based on a hybrid analogue-digital system [15] and has a PID structure. For the experiments described in this paper, this controller was replaced entirely by a new Digital Plasma Control System, DPCS [13]. This system has 192 analogue inputs and 64 analogue outputs in a VME environment. The Single Instruction Multiple Data architecture of the high-speed calculator provides a maximum computation speed of 2.5GFLOPS, of which a sustained speed of 0.8GFLOPS is obtained with the particular control system implementation. The DPCS has a cycle time of 0.110msec in these experiments and a typical latency delay of 0.070msec.

The parameters under feedback control, illustrated in Fig. 2, can be arbitrarily chosen. For these experiments, we retained those used in the model validation [10-12], namely the plasma current (Ip), the vertical position times the instantaneous plasma current (zIp), the inboard-outboard flux imbalance (P_VERT) and two linear estimators of the separatrix curvature on the inboard and outboard sides of the plasma respectively (TRI_IN and TRI_OUT). The latter two parameters together regulate the plasma shape.

For the PID controller design a simplified set of models was used. For plasma current control, a simple self-inductance was used to scale the flux control on the inboard mid-plane. For the vertical control, a rigid current model of the vertical plasma displacement was used, combined with empirical tuning. For the remaining three parameters a plasmaless low-frequency estimate of the plant was used. Such an approach was considered inadequate for the design of an advanced controller and the CREATE-L model of TCV was developed.

The CREATE-L linearised model of the TCV tokamak is expressed in state-space form as:

$$dx/dt = \mathbf{A}\,x + \mathbf{B}\,u \qquad (1)$$

where x is the state vector consisting of currents in the PF coils and in the passive structures, and u is the input vector, namely the linearised PF coil voltages. For the TCV model the state vector x has 75 elements. The matrix determining the poles of the system is **A** and the matrix describing the coupling between the applied voltages and the internal states is **B**. The states determine the output parameters y, which include the linearised variations of the field and flux measurements and the poloidal field coil currents, using the standard output equation:

$$y = \mathbf{C}\,x \qquad (2)$$

where **C** is the state-to-output matrix.

From the point of view of the controller designer, the most important property of the overall system is its vertical position instability in open loop, represented in the model by a single unstable pole. The large number of 18 separate inputs also provides an interesting challenge. The large power handled by the TCV tokamak PF power supplies (up to 100MW) is much less than for the ITER design but already does not permit any uncontrolled tuning. For that reason, empirical tuning is always a cautious and therefore time-consuming step-by-step method on present tokamaks.

3. CONTROLLER DESIGN TARGETS

The controller designer has to be presented with predetermined design targets. We chose the tracking of separate square pulse reference excursions as a suitable test. Results have been presented previously [14] for a PID controller and a limited, up-down symmetric plasma which was centred at the midplane. The performance proved to be acceptable, although the decoupling, as well as the pulse responses, was far from perfect.

A new exercise was performed with the same PID controller assuming a nominal plasma above the midplane, weakly shaped and up-down asymmetric, with parameters: κ_{95}=1.46, δ_{95}=0.28, R_p=0.89m, I_p=200kA, q_a=7.3, and a growth rate of 60/sec. This plasma is shown in Fig. 1.

When operating the plasma above the midplane, the natural decoupling between the vertical movement and the other 4 control parameters is lost. Figure 3 shows the performance of the PID controller for this exercise. This controller had not been retuned or redesigned for this plasma and this performance should not be considered as being in any way representative of what could be obtained with a retuned PID controller or a PID controller tuned on a more accurate model. The choice of the parameters to be controlled was also not in any sense optimised for this experiment.

A feature of TCV is that with the number of controlled parameters significantly less than the number of PF control coils, the currents in the control coils which can satisfy zero error in the control parameters represents a large "null" space. This null space is

in turn controlled by specifying the PF coil currents in advance and requesting the minimum coil current modifications to satisfy the control parameter regulation. Different controllers will satisfy the regulation problem with different usage of this null space, provoking different changes to the plasma shape within the control of our restrictive control parameter set. This problem is left to the controller to optimise and was not part of the design target.

Figure 4 shows reconstructed shape and position parameters during the reference excursions of the 5 controlled parameters (also labelled B-F in Fig. 5). In Fig. 3 the response of P_VERT to a step reference is reasonably rapid although the amplitude of the response is about 15% in excess of the reference pulse. During this pulse there is coupling with the TRI_OUT control parameter and only transient coupling to Ip. The parameter zIp is largely unaffected, since the response of the controller generates no radial field on axis. The reconstructed responses show that this excursion ('B') causes the radial position to move outward with a small affect on κ and δ. The second pulse, TRI_OUT, causes very little response and couples somewhat to P_VERT. Equilibrium 'C' has a modified curvature at the top of the plasma. A step increase in κ and a step decrease in δ are observed. The third pulse, TRI_IN, has 50% of the required response and also couples somewhat to P_VERT. Equilibrium 'D' has a straighter inner part of the contour and modified X-point configuration. A step increase in both κ and δ are observed in the reconstructed responses. The fourth pulse, zIp, produces a fast response in zIp which settles quickly and accurately to the reference level, but which also produces a 60% overshoot and strong transient coupling to TRI_OUT and TRI_IN and to a lesser extent to Ip. Equilibrium 'E' is at a higher vertical position, but the shape has also changed slightly. The coupling is reflected in the reconstructed shape and position parameters. Finally, the pulse to Ip provides an excellent tracking response Ip itself but some coupling to TRI_OUT and TRI_IN. The major weaknesses of this controller are therefore, in order, the tracking response of TRI_OUT, the coupling between zIp and the shape parameters, and the steady state tracking error in the P_VERT response.

Since this was the first attempt a set of relatively conservative design goals were chosen for the new controller:

- The controller should stabilise the reference plasma and similar weakly shaped, symmetric, plasmas positioned at the midplane. To check this, simulations were performed using the plasma models appropriate to different equilibria.

- The controller must be designed to tolerate uncertainties in the PF coil currents with respect to the nominal model. Departures of the coil currents from the nominal equilibrium should not be compensated, since the coil currents do not have an error in the sense that they ought to be exactly those programmed.

- The controller has to be robust to unpredictable behaviour of the PF coil supplies. Although the power supplies operate in all 4 quadrants, they have to be instructed to cross zero current. If such a command is not given, the crossing does not occur and the power supply appears to be inactive (saturation at zero current.)

- The controller has to be insensitive to real experimental noise in the control parameter estimators. Data from typical discharges with the noise to be expected were available during the controller design.

- The closed loop bandwidth was allowed to be relatively low to allow for lower power consumption and minimise any possibility of voltage saturation.

The main design challenge was to demonstrate that the controller could function given real conditions in the tokamak operation, not included explicitly in the linearised model. We return to this question both in the design methodology and in the results discussion.

4. CONTROLLER DESIGN

The main objective of the controller is the robust stabilisation of the plasma vertical position and this is particularly demanding. A vertical shift of the plasma in the vessel of just a few centimetres can modify the phase responses of the transfer functions between the voltages in the coils near the plasma and the vertical position by up to 180°; this could even lead to closed loop instability. This strongly nonlinear behaviour of the plant makes it difficult to design a MIMO (multi-input multi-output) controller in just one step. Indeed, because of the conservativeness of almost all the MIMO controller design techniques with respect to structured uncertainties, it is hard to find a controller which both stabilises all the linearised models in the considered working envelope and guarantees the desired performance. For this reason we split the controller design into two steps. In the first step we stabilise the vertical position using only some of the PF coils, namely those not too near to the plasma. Afterwards, on the basis of the stabilised plant, we design a second controller able to guarantee the decoupling among the control parameters with acceptable dynamics, using the remainingcoils.

A SISO (single-input single-output) controller was designed for the control of the vertical position. This used a simple PID controller, so as to avoid the conservativeness problems as discussed above. The control of the other parameters calls for a MIMO approach because of the strong output coupling between the control parameters. For this second step we chose the H_∞ framework. Using this technique it is possible to specify many different constraints on the desired closed loop response of the system. The open loop plant model used in the design was described in Section 2 and consists of the CREATE-L plasma model, the power supplies, and the DPCS sampling and latency times.

4.1 The PID design

The first step was the derivation of a simplified vertical model from the full linear model to design the PID controller. The nominal plasma we considered is not centred, but is shifted about 11 cm above the midplane; for this reason, the coils we chose for the vertical stabilisation are not symmetric with respect to the midplane. Only eight coils were used: E3, E4, E6, E7; F3, F4, F6, F7 (Fig. 1). The E5 and F5 coils were not

employed because their closeness to the plasma centre makes the sign of the gain (with respect to the vertical position) uncertain. As a consequence of this, if these two coils were also used, the closed loop system could exhibit poor stability margins.

The eight chosen coils were grouped together, to obtain a SISO system with an equivalent coil as input and the vertical position as output. The coils were weighted differently, according to their resistances. A balanced realisation of the stable part of the system was obtained and model reduction used to reduce it to 6th order [16]. The model was then augmented with a Padé approximation of the time delay due to the DPCS and to the continuous time to discrete time conversion of the controller.

The robust stabilisation problem was made more challenging by the non-minimum phase zeros of the plant and by the high variability of the growth rate. In fact, the growth rate of the unstable mode for the plasmas considered in this paper varies from up to 300 s^{-1}, according to the position of the plasma in the vessel and the field curvature of the equilibrium considered.

Based on the reduced order model, a PID controller was designed using a standard frequency domain design method. In particular the gain and phase margins were made sufficiently high in order to guarantee the stabilisation of a number of models suitably chosen in the assumed working envelope.

In Fig. 6 the Nichols diagrams of three different open loop transfer functions are shown, namely the cascade of the designed PID controller and the vertical model of three different plasma equilibria in the assumed working envelope. In particular we chose the nominal plasma configuration, i.e. a limited plasma shifted about 11cm, a diverted plasma with the same vertical shift, and a limited centred plasma, which was more unstable than the nominal one.

4.2 The H_∞ controller design

Once designed, this PID controller was absorbed into a generalised plant. This plant was then used to design the H_∞ shape controller. The H_∞ controller inputs are the remaining four control parameters, i.e. TRI_IN, TRI_OUT, Ip and P_VERT. Its outputs are the voltages of the coils that are not used by PID, i.e. E1, E2, E5, E8; F1, F2, F5, F8; OH1, OH2. This was a design choice made only for this first attempt. For further details on the H_∞ design approach, the interested reader can refer to [7]. For the TCV tokamak, the augmented plant used in the H_∞ framework to design the controller is shown in Fig. 7. In this Figure:

- P is a reduced order model of the plant (plasma and actuators) including the PID stabilising controller; the model order reduction introduced a model uncertainty;
- Δ_c and W_{del} together characterise the total model uncertainty. The parameter Δ_c is is an element of a set of transfer functions and parametrizes the model variations of the nominal design model. Its structure is an unknown full block complex matrix with $\|\Delta_c\|_\infty \leq 1$;

- W_{del} is a frequency dependent diagonal weight, obtained by comparing full order models of different plasma configurations and the reduced order design model. These diagonal weights were chosen equal for each of the inputs; their Bode magnitude diagram is shown in Fig. 8;
- W_p is used to ensure the desired time behaviour to each of the four controlled outputs. It is diagonal and each non-zero entry has the form:

$$W_{pi} = K_i \frac{1+s\tau_i}{s};$$

- These weighting functions are shown in Fig. 9. They have been tuned through a trial and error procedure based on simulations;
- W_{cur} is a scalar diagonal weighting matrix used to limit the maximum amplitude of the coil currents. These weights were chosen to be equal for the various coils and after a tuning they were fixed at 0.4;
- W_{cont} is a diagonal matrix frequency dependent weighting function which penalises the high frequency control effort in order to limit the bandwidth of the controller. The Bode diagram shown in Fig. 10 refers to the OH and F coils; the corresponding weighting function for the E coils has twice the magnitude at all frequencies;
- W_{out} is a scalar diagonal matrix used to scale the reference inputs on the four controlled parameters. These scalars have been tuned by a trial and error procedure: $W_{out} = \text{diag}\{10^{-6}, 10^{-6}, 10^{-6}, 5\}$.

The solution to the H_∞ problem was found using the μ-toolbox of the Matlab computer language [17].

The two controllers were eventually grouped together and converted to discrete time using the Tustin bilinear approximation and the appropriate sampling time of 110μs.

4.3 Switching algorithm

The issue of switching between the PID controller used for the initiation and extinction phases, and the H_∞ controller has been considered, and a simple algorithm was developed to avoid large transients. The digital implementation of both the PID and the H_∞ controllers are in state space form:

$$\begin{aligned} \boldsymbol{x}_P[n+1] &= \mathbf{A}_P \boldsymbol{x}_P[n] + \mathbf{B}_P \boldsymbol{u}[n] \\ \boldsymbol{y}_P[n] &= \mathbf{C}_P \boldsymbol{x}_P[n] \end{aligned} \tag{3}$$

where $\boldsymbol{x}_P[n]$ is the state vector at sampling instant n, $\boldsymbol{u}$ and $\boldsymbol{y}$ are the control parameter error vector and control coil demand voltage vector respectively, and the subscript 'P' represents the PID controller (alternatively 'H' for the H_∞ controller). The controller dynamics are then defined by the state space matrices **A**, **B** and **C** in a similar manner as in Eqs. 1 and 2. When switching between the two controllers, the state space matrices implemented in the DPCS are changed and the state vector initialised.

At any switching instant, the new controller states were set by assuming an initial value of zero and then "winding on" the controller assuming that all the controller

inputs were constant in time. For example to switch to the H_∞ controller at a sampling instant k, the controller state would be initialised to

$$x_H[k] = \left(\sum_{i=0}^{c-1} \mathbf{A}_H^i \right) \mathbf{B}_H u[k] \tag{4}$$

where c is the number of wind on cycles. Winding on the state like this avoids the main transient part of the step response of the controller. For the PID it was found that 15 wind on cycles gave good results and that for the H_∞ controller 5 wind on cycles gave good results. Both switches used 5 cycles of winding on in the discharge presented. In order to remove any DC step differences, the programmed demand voltages were incremented by the difference between the two controller outputs, removing any discontinuity in the demand signals, i.e.

$$y[k] = \mathbf{C}_H x_H[k] + \varepsilon \tag{5}$$

where y is the power supply demand signal and ε is the difference $\varepsilon = y_P[k] - y_H[k]$. The latter measure might in fact be unnecessary. The switching is thereby reduced to a single matrix multiplication of the winding on operating on the last error, followed by a subtraction. The switching causes a delay of a few microseconds in the DPCS, which is recovered in the next cycle.

5. RESULTS

The new controller was implemented in the DPCS. Initially this was made to shadow the analogue control system during the operation of a single tokamak discharge, including the switching between PID and H_∞ controllers during the flat top. This open loop verification of the controller and switching algorithm confirmed the absence of implementation problems. Following this single test discharge (#14192), the DPCS was given control of all of the TCV control system and the first successful closed loop operation of this controller was achieved (#14193). The switching produced no visible transient effects on the overall closed loop control.

Figure 5 illustrates two of the controlled variables, namely the plasma current and the vertical position, together with their reference variables. The closed loop stability and the absence of transients during the switching marked by the vertical lines are already clear from this simple result. The times of the square pulse reference excursions are marked 'B'-'F' with 'A' being the reference equilibrium.

Figure 11 shows the details of the behaviour of the 5 controlled parameters during this experiment and can be compared directly with Fig. 3. The response to the first reference excursion, P_VERT, is slower than for the PID, but the cross-coupling is less and the response amplitude is correct. The second reference excursion, TRI_OUT, now has the correct sign and the correct amplitude and also provokes less cross-coupling than the PID. The third reference excursion, TRI_IN, has the correct amplitude and minimal cross-coupling. The fourth reference excursion, zIp, shows no cross-coupling at low frequency but a significant transient overshoot due to the PID design and speed of response. The fifth reference excursion, Ip, shows a good response and only a little cross-coupling to the radial position P_VERT. The decoupling performance is therefore superior to the PID for all responses and all cross-couplings. The response performance is not yet optimal for zIp for normal

tokamak operation since the extremely fast response provokes a large overshoot, even larger than the PID and significant transients in the other parameters. It is the choice of the controller designer to balance the speed of response against the overshoot. The tracking and decoupling benefits of the H∞ controller have been clearly demonstrated.

The experiment equilibrium was not identical to the design equilibrium leading to an error in the model. Also shown in Fig. 11 is a simulation of the H_∞ controller using the design model of the plant. A second model was created from the experiment equilibrium to compare with the design model. Simulating the effect of the reference excursions on the experiment equilibrium model gave better agreement. The similarity demonstrates the performance robustness to some parameter variations and the ability of the method and model to predict the tokamak behaviour.

The output voltages for 4 selected power supplies are compared in Fig. 12 for the two controllers. There is no significant difference between the control voltages used, although different coils respond differently to different controller error inputs. The improved decoupling has therefore not been achieved by increasing the control voltages.

We have inspected the PF control power used by the two controllers on the E and F coils of TCV, excluding the response to the Ip and zIp reference excursions (Fig. 13). The peak absolute value of power on each of the coils is similar for the two controllers. The variation in responses is more marked for the F coils where the H_∞ controller uses up to a half or double the power of the PID controller. In overall terms the use of the H_∞ controller did not require more power.

The voltage transients during the controller switching are presented in Fig. 14. The transients are of the order of 8% of the full-scale power supply voltages at most. The transient at t=0.803s is due to the start of the plasma current ramp-down.

During the first test discharge, the voltage demand signals drove some of the PF coil currents to zero. These particular power supplies have to be instructed to cross through zero current and inverse the sign of the delivered current and this was not done during these transients. The power supplies were therefore acting in current saturation, although at zero rather than maximum current. Figure 15 illustrates this feature for some power supplies. The fact that the controller maintained stability and performance with this current saturation is encouraging.

6. DISCUSSION

In this work we have demonstrated the validity of a design approach using an advanced controller for the TCV tokamak. The CREATE-L plasma equilibrium response model had been previously experimentally validated on TCV. This model was presented to controller design engineers unfamiliar with the operation of TCV, together with a set of design targets and a model of the controller input noise, to develop a robust advanced controller using the H_∞ technique. The controller performance was exhaustively tested on a set of models which represented the likely spread of the tokamak plasma parameters. This controller was imported directly into

the TCV digital plasma control system and switched into operation during the flat top of a tokamak discharge. In this first discharge it delivered the design performance which was considerably better than the performance of a multivariable PID controller.

Extensions to this work will include the implementation of a full H_∞ controller, the incorporation of a technique to reduce the total power requirement during the control actions, essential for the ITER tokamak performance, and a verification of the effects of poloidal field coil voltage and current saturation. The performance of the controller will be further tuned to the TCV operational requirements.

ACKNOWLEDGEMENTS

It is a pleasure to acknowledge the support of the TCV team during the execution of this work, as well as the motivation provided by Profs. R. Albanese and E. Coccorese as well as colleagues in the ITER JCT and NET teams. This project was originally proposed for TCV by Dr. F. Engelmann as R&D support for the ITER design. Two of the authors (MA, FV) acknowledge mobility support from Euratom. The work was partly funded by the fonds national suisse de la recherche scientifique.

REFERENCES

[1] A. OGATA, and H. NINOMIYA, "Use of Modern Control Theory at Neutral Beam Injection," *Proc. 8th Symp. Engineering Problems of Fusion Research, San Francisco, USA, November 1979*, Vol. IV, p. 1879 (1979).

[2] C.E. KESSEL, M.A. FIRESTONE, and R.W. CONN, "Linear Optimal Control of Tokamak Fusion Devices," *Fusion Technology,* Vol. 17, p. 391 (May 1990).

[3] R. ALBANESE et al., "Plasma Current, Shape, and Position Control in ITER," *Fusion Technology*, Vol. 30, (1996).

[4] A. PORTONE, et al., "Dynamic Control of Plasma Position and Shape in ITER," *Fusion Technology,* Vol. 32, p. 374 (1997).

[5] M.M.M. AL-HUSARI et al., "Vertical Stabilisation of Tokamak Plasmas," *Proc. 30th IEEE Conf. Decision and Control, Brighton, England, December 1991,* p. 1165-1170 (1991).

[6] PORTONE, A., "Modelling and Control of Tokamak Plasmas in Fusion Devices," PhD Thesis, University of London, Imperial College of Science, Technology and Medicine (1994).

[7] G. AMBROSINO et al., "Plasma Current and Shape Control in Tokamaks using H_∞ and μ-synthesis," *Proc. 36th IEEE Conf. Decision and Control, San Diego, USA, December 1997,* p. 3697 (1997)

[8] P. VYAS., A.W. MORRIS and D. MUSTAFA, "Vertical Position Control on COMPASS-D," *Fusion Technology,* Vol. 33, No. 2, pp. 97-105 (March 1998)

[9] R. ALBANESE and F. VILLONE, "The linearized CREATE-L plasma response model for the control of current, position and shape in tokamaks," *Nuclear Fusion*, Vol. 38, No. 5, pp. 723-738 (May 1998)

[10] F. VILLONE, P. VYAS, J.B. LISTER and R. ALBANESE, "Comparison of the CREATE-L Plasma Response Model with TCV Limited Discharges," *Nuclear Fusion*, Vol. 37, No. 10, p. 1395 (1997)

[11] P. VYAS, F. VILLONE, J.B. LISTER and R. ALBANESE, "The Separatrix Response of Diverted TCV Plasmas Compared to the CREATE-L Model," *Nuclear Fusion*, Vol. 38, No. 7, p. 1043 (1998)

[12] A. COUTLIS et al., "Measurement of the Open Loop Plasma Equilibrium Response in TCV," *Report LRP 611/98, CRPP, EPFL, Lausanne, Switzerland* (June 1998)

[13] J.B. LISTER, M.J. DUTCH, P.G. MILNE, R.W. MEANS, "A High-Performance Digital Control System for TCV," *IEEE Trans. Nucl. Sc.,* Vol. 45, No. 4, pp. 2044-2051 (1998).

[14] J.B. LISTER et al., "The Control of Tokamak Configuration Variable Plasmas," *Fusion Technology*, Vol. 32, pp. 321-373 (November 1997)

[15] P.F. ISOZ, J.B. LISTER and P. MARMILLOD, "A Hybrid Matrix Multiplier for Control of the TCV Tokamak," *Proc 16th Symp. Fusion Technology, London, UK, September 1990*, Vol. 2, pp. 1264-1267 (1990)

[16] M. GREEN, D. J. N. LIMEBEER, *Linear Robust Control*, Prentice Hall, Englewood Cliffs, NJ, 1995.

[17] J. B. BALAS, J. C. DOYLE, K. GLOVER, A. PACKARD, R. SMITH, *μ-Analysis and Synthesis Toolbox*. The MathWorks, Inc. and Musyn, Inc., 1991

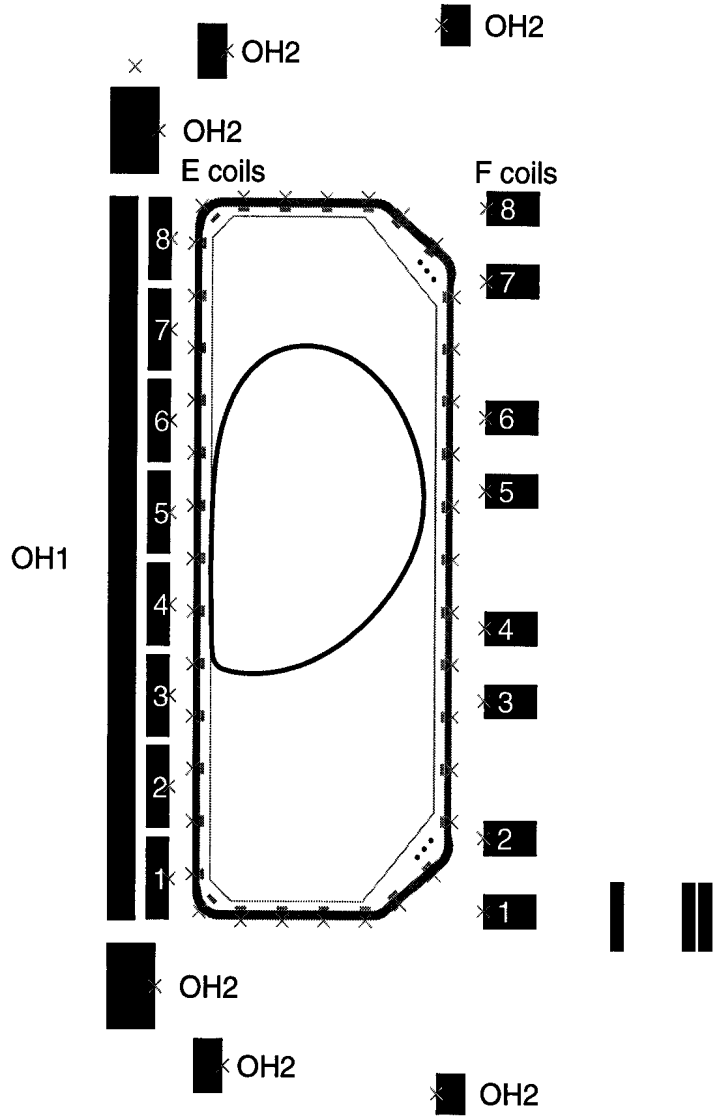

Figure 1. The TCV vessel, the poloidal field coils and the nominal separatrix contour shape. The magnetic diagnostics are shown as bars (poloidal field probes) and crosses (poloidal flux loops).

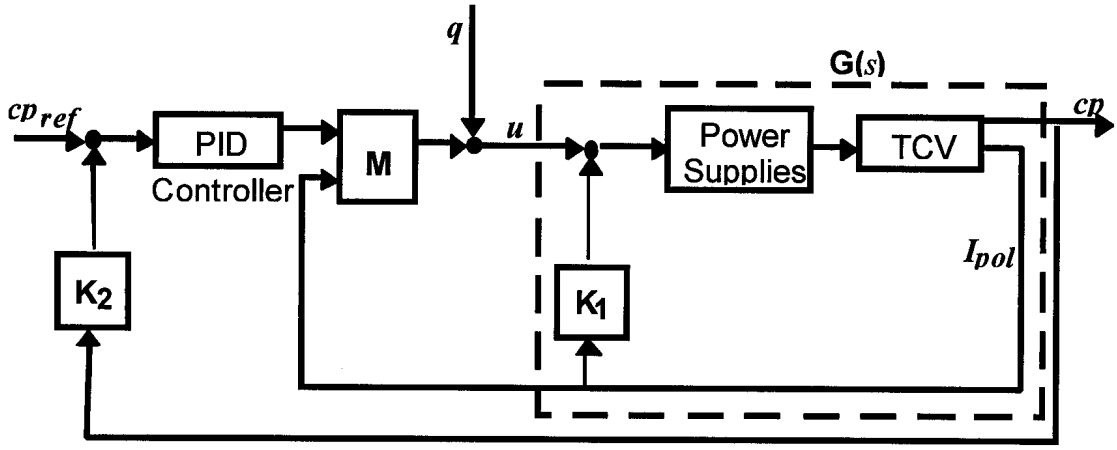

Figure 2. Schematic Diagram of the TCV feedback control loop. The 'TCV' block represents the responses of the plasma control parameter (***cp***) and the coil currents (***Ipol***) to voltages applied on the poloidal field coils. The signal ***u*** represents the power supply input signal and ***q*** represents an external stimulation signal. The system **G(*s*)** represents the open loop plant from the power supply inputs to the control parameters and includes the effect of a diagonal current feedback matrix in the power supplies (**K1**). The feedback system consists of a PID controller and feedback matrices **M** and **K2**.

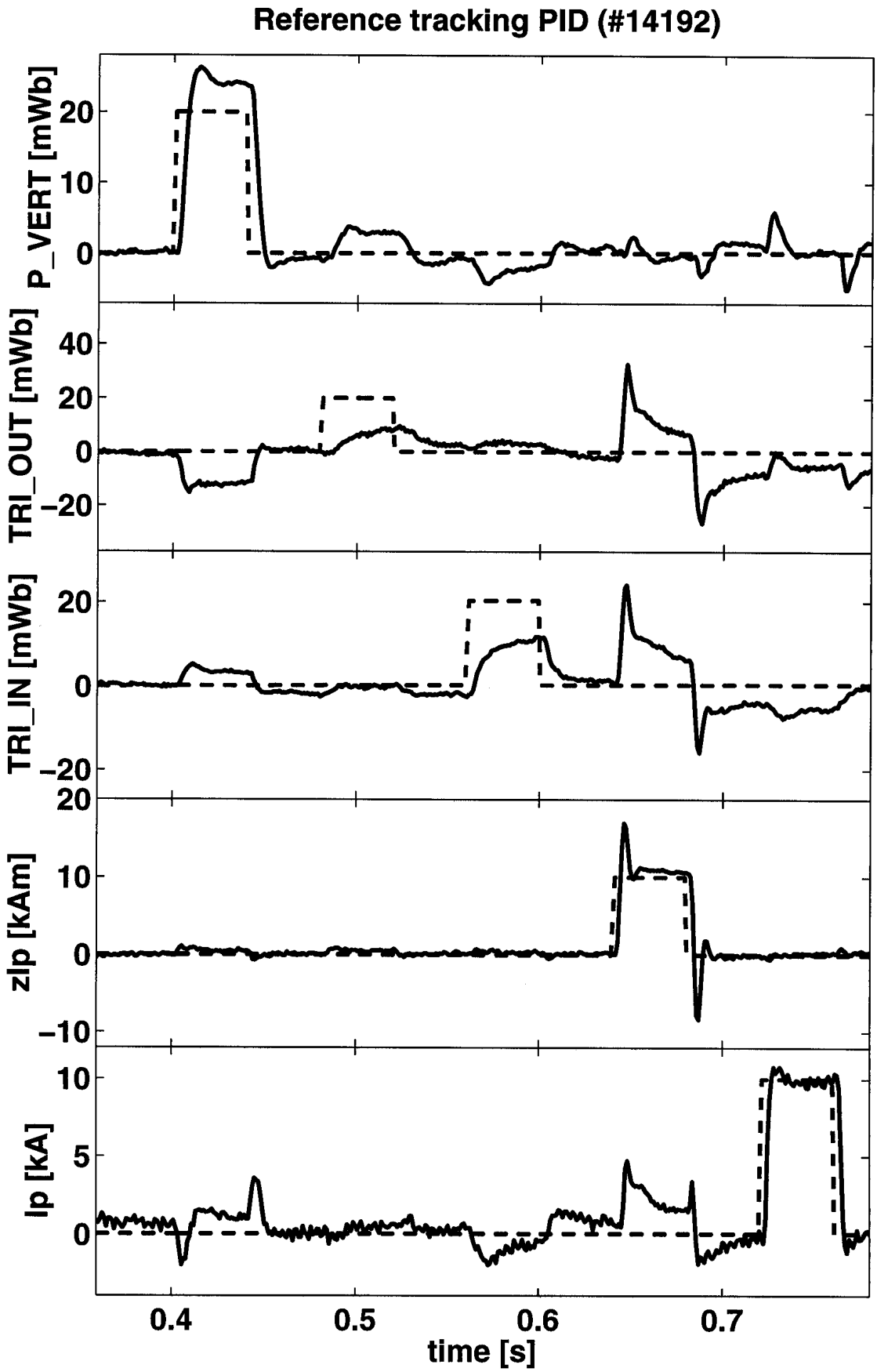

Figure 3. The evolution of the control parameters during a discharge controlled by the hybrid PID controller. The references are shown as dashed lines.

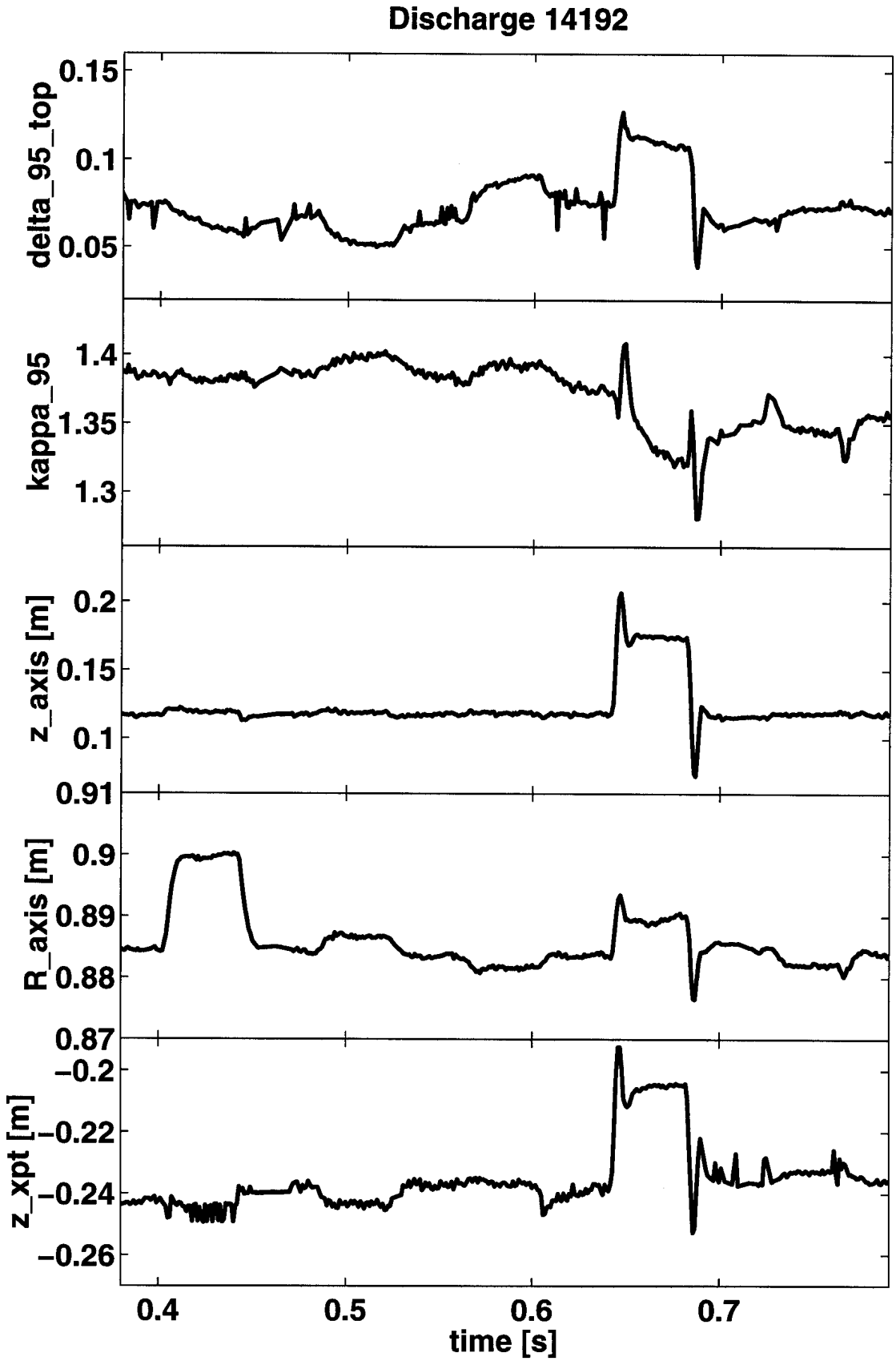

Figure 4. Reconstructed plasma parameters. From top to bottom: upper triangularity at the 95% flux surface, elongation at the 95% flux surface, vertical and radial position of magnetic axis respectively, and vertical position of plasma X-point.

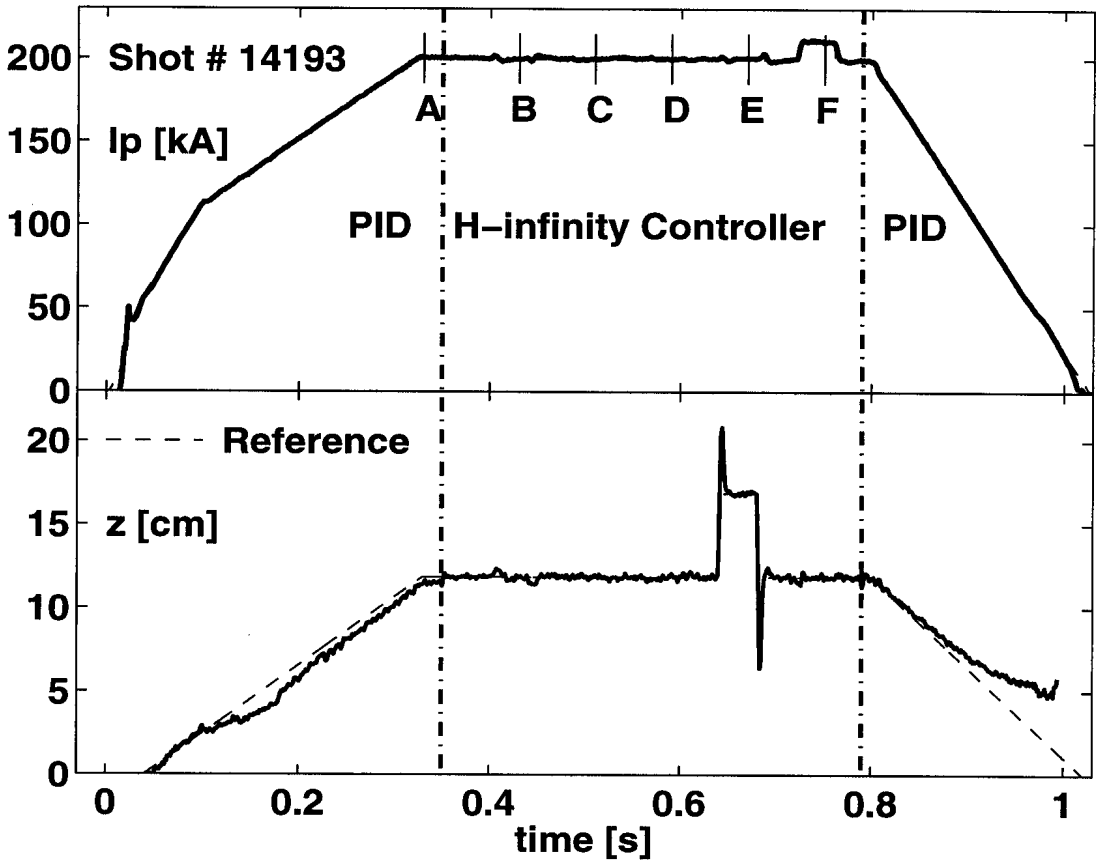

Figure 5. Evolution of the plasma current, Ip, and the vertical height (z) for the full discharge. The reference waveforms are indicated as dashed lines. The switching between controllers is indicated as vertical lines. The times at which the equilibria are stationary during the reference pulses are indicated as 'B' to 'F', the reference equilibrium is 'A'.

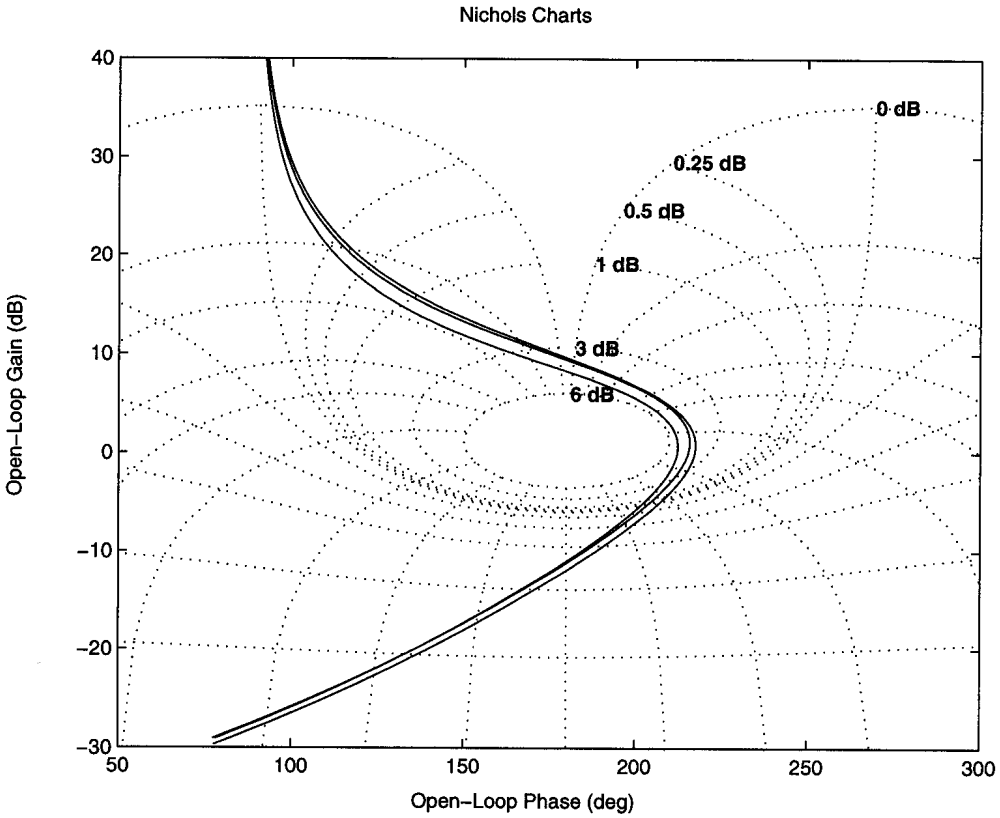

Figure 6. The Nichols plots of the open loop gains obtained considering three different plasmas and the PID controller. The controlled variable is the vertical position.

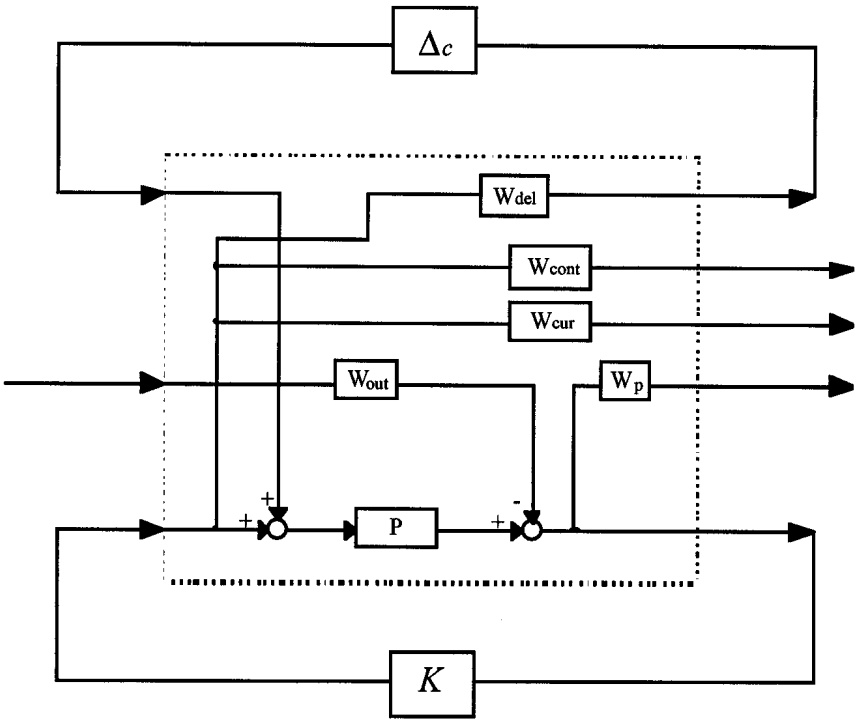

Figure 7. The framework for the design of the H_∞ shape controller.

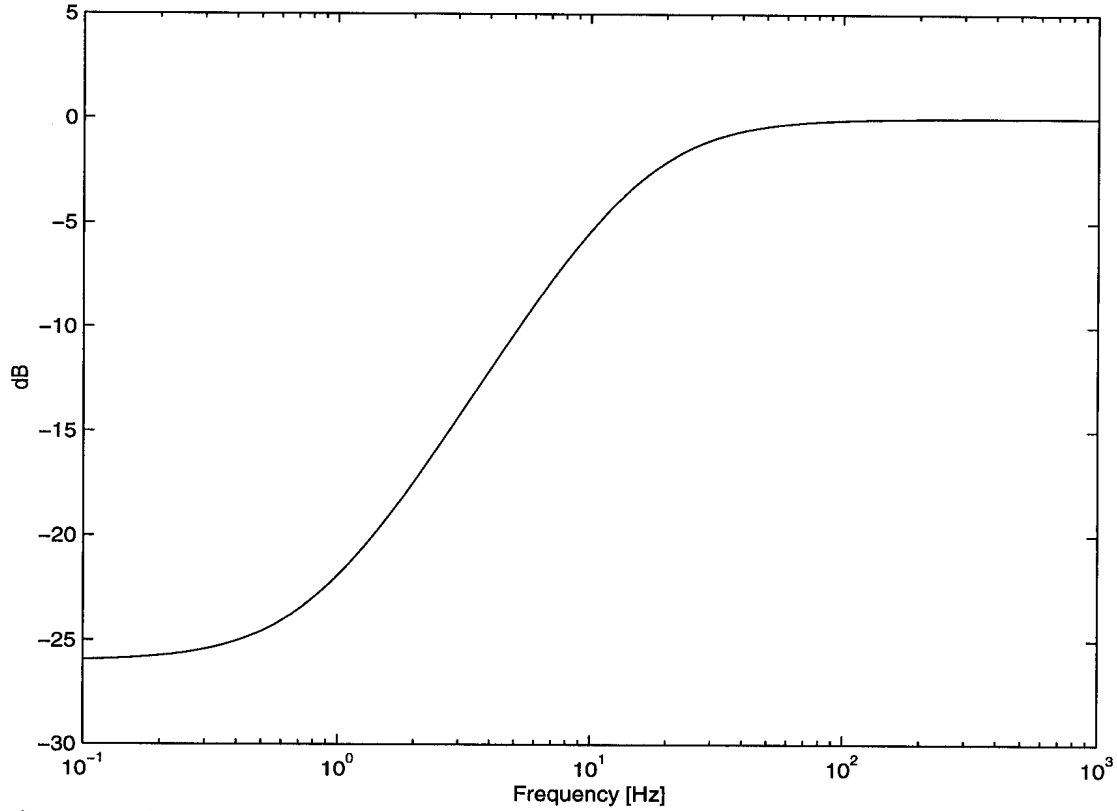

Figure 8. The multiplicative uncertainty at the input of the plant (equal for each of the coils).

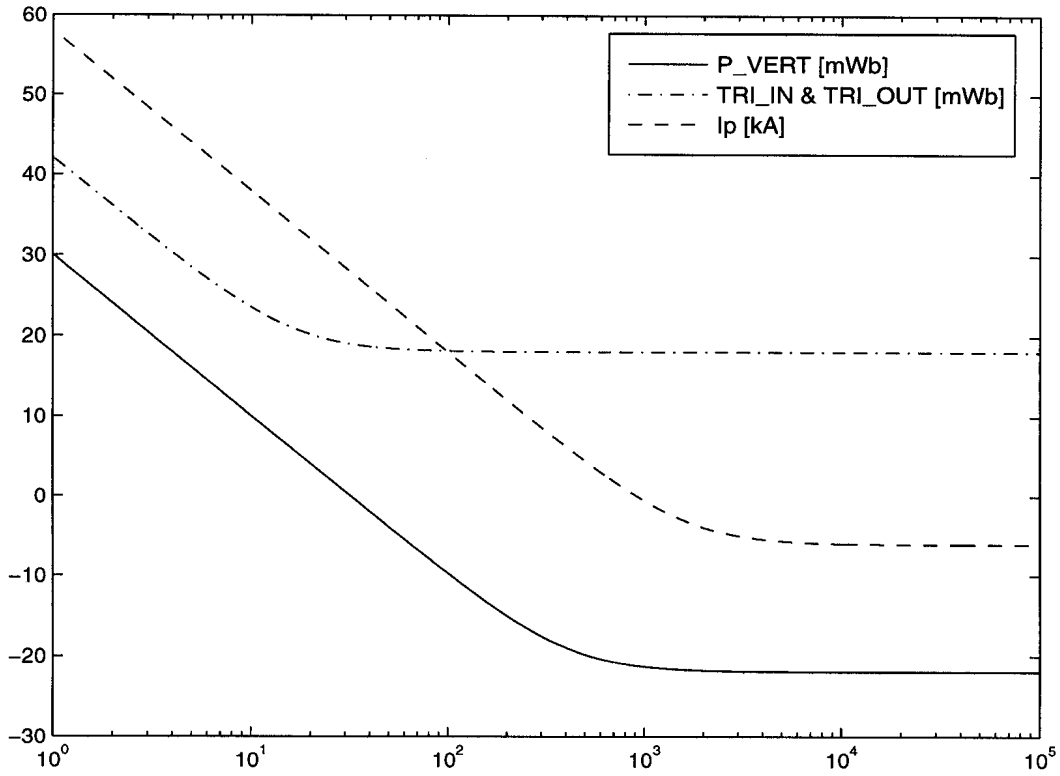

Figure 9. The weight on the four parameters controlled by the H_∞ controller.

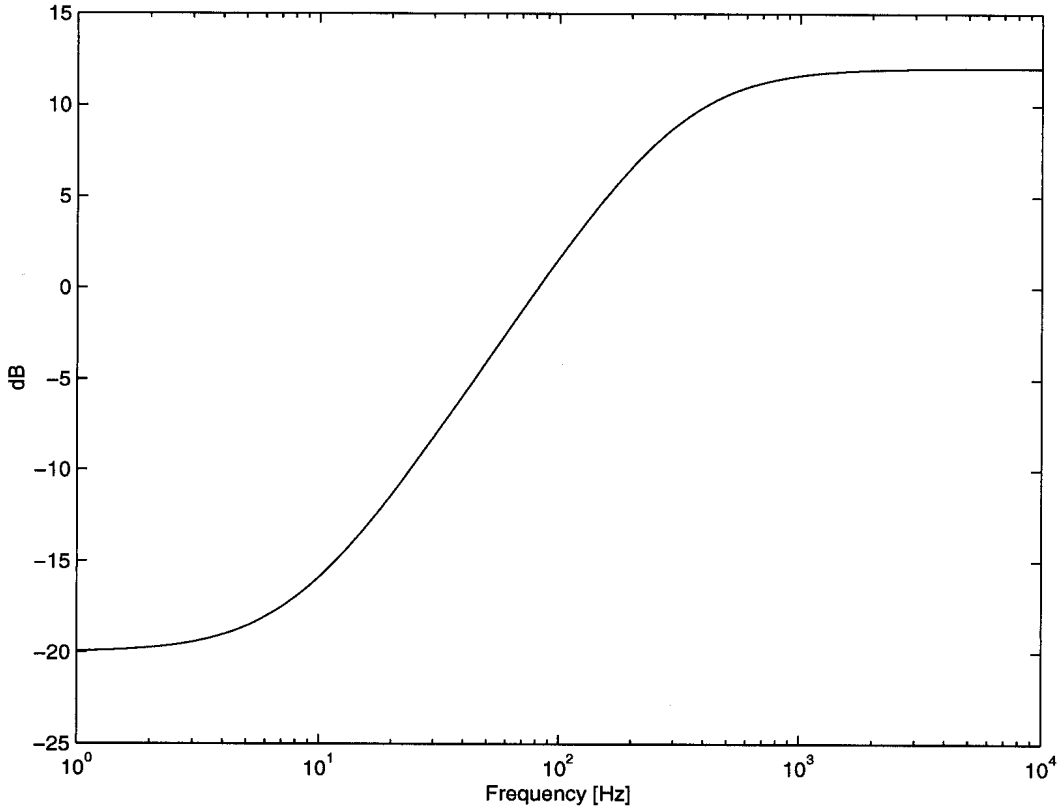

Figure 10. The filter used to weight the control voltages.

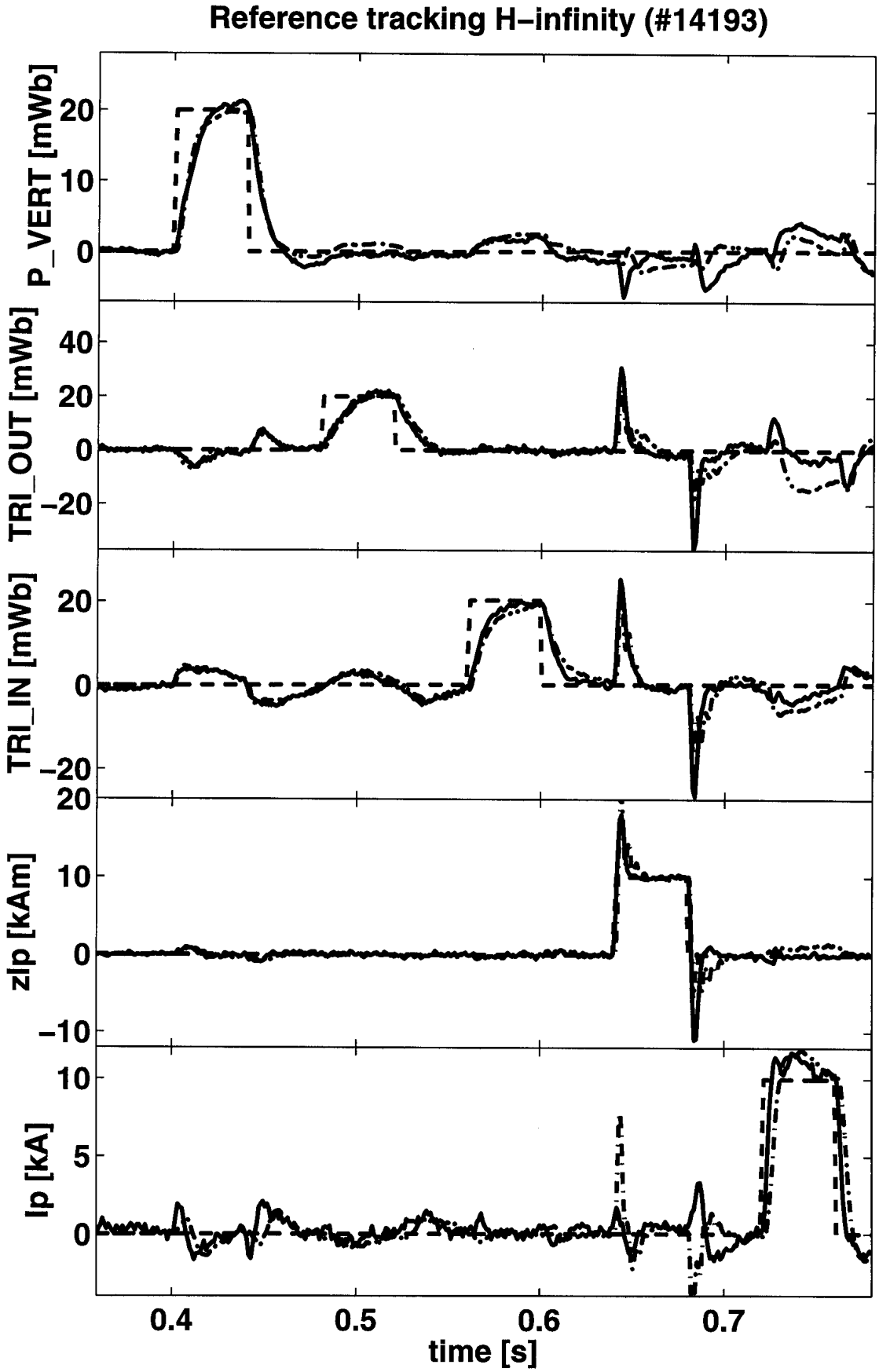

Figure 11. The evolution of the control parameters during a discharge controlled by the H_∞ controller. The references are shown as dashed lines and the modelled response is shown as dash-dotted lines.

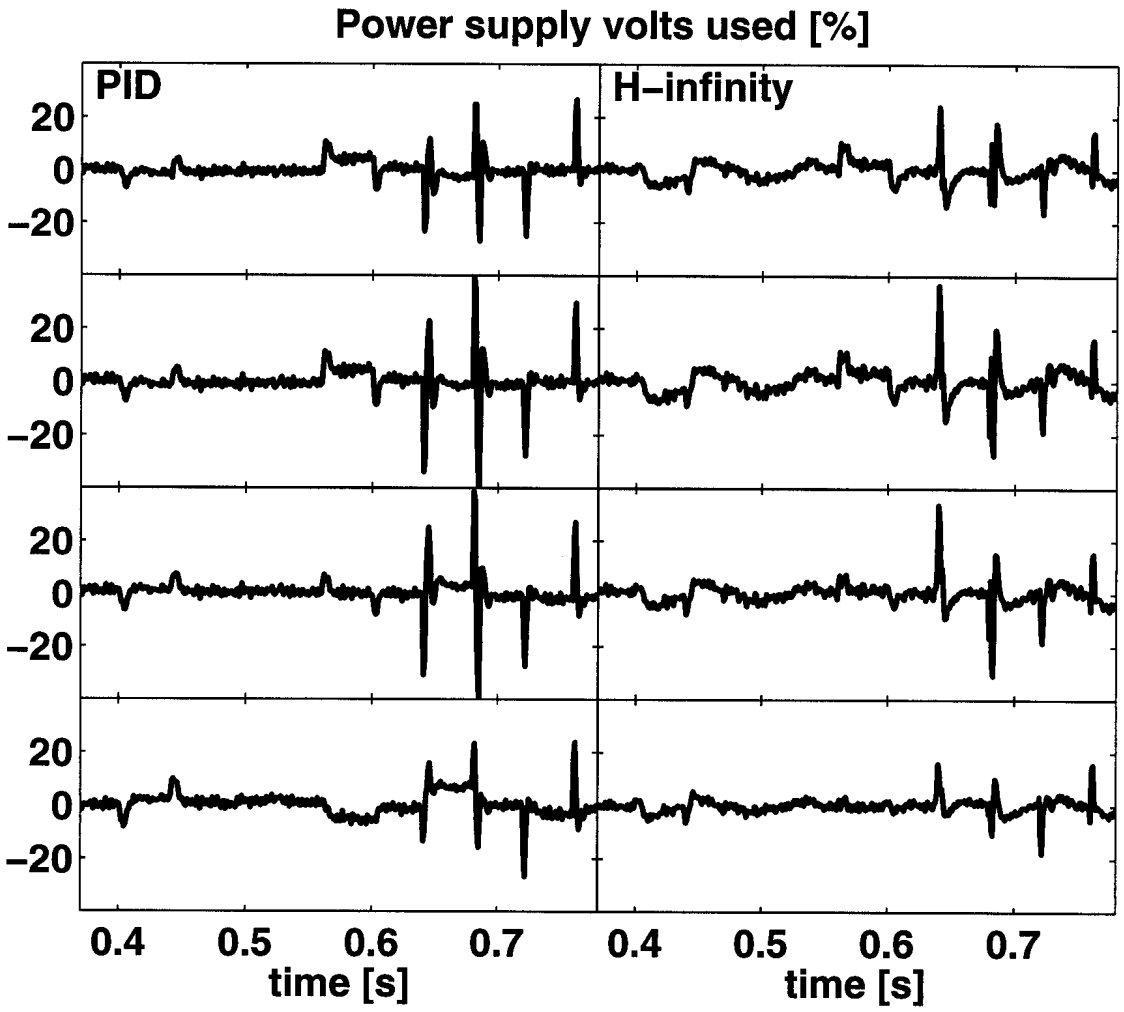

Figure 12. Comparison between the PF coil voltages used by the PID controller and the H_∞ controller.

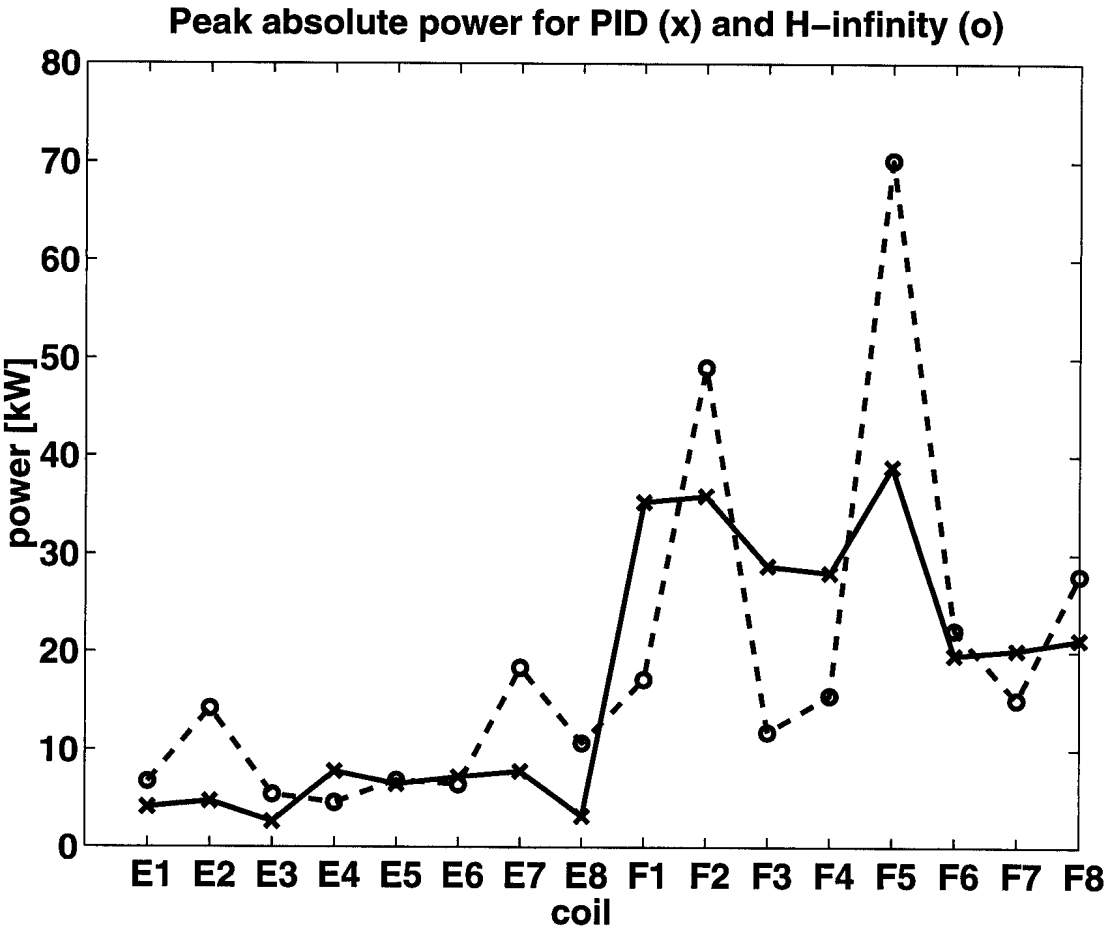

Figure 13. Comparison of peak absolute value of power applied on each individual coil with the PID controller ('x') and the H_∞ controller ('o'). The zIp and Ip reference excursions are excluded from this calculation. The peak absolute value of the sum of the power across all the E and F coils is 115kW for the PID controller and 51kW for the H_∞ controller.

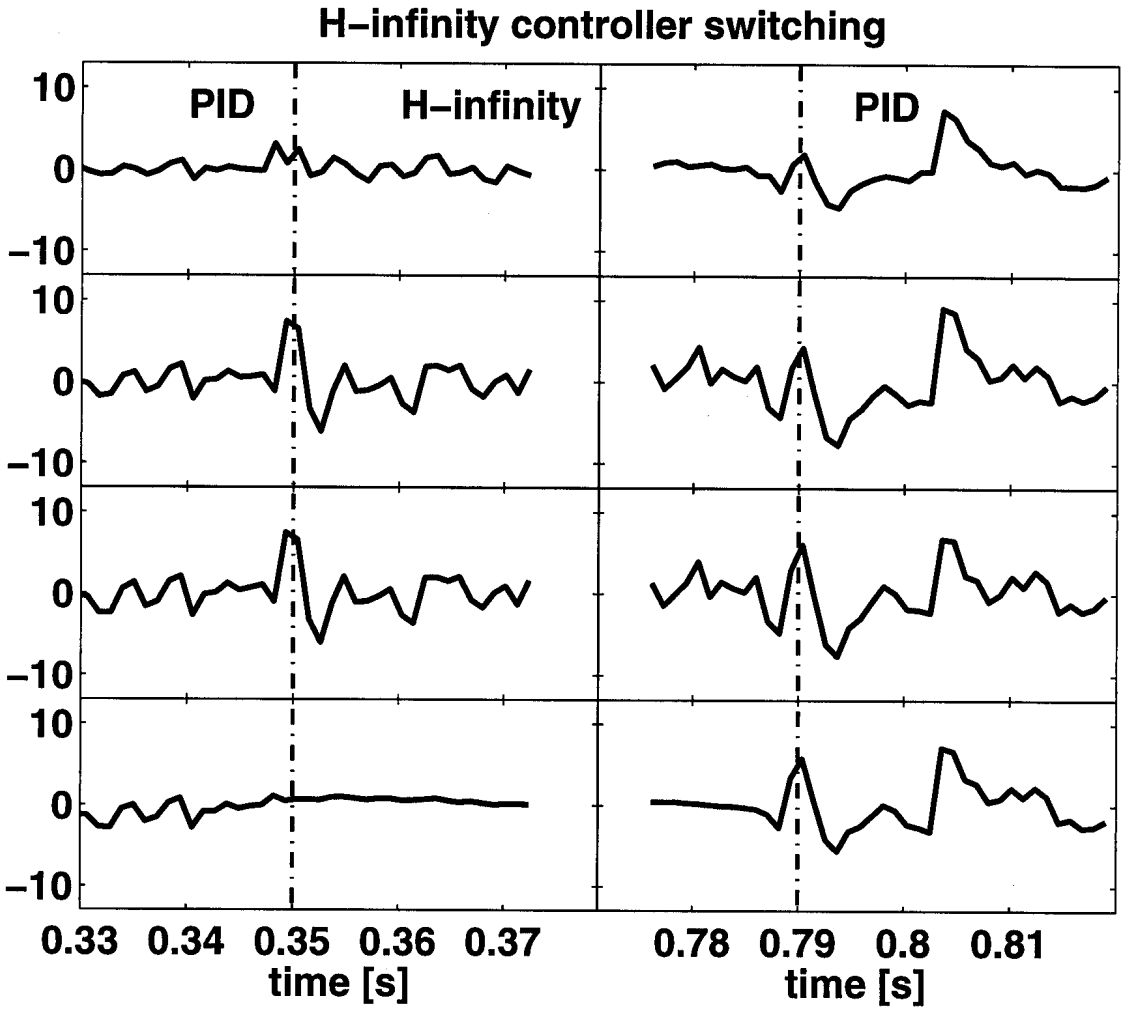

Figure 14. Variation of some of the power supply demand voltages during the controller switching. Voltages are expressed as a percentage of the full-scale volts.

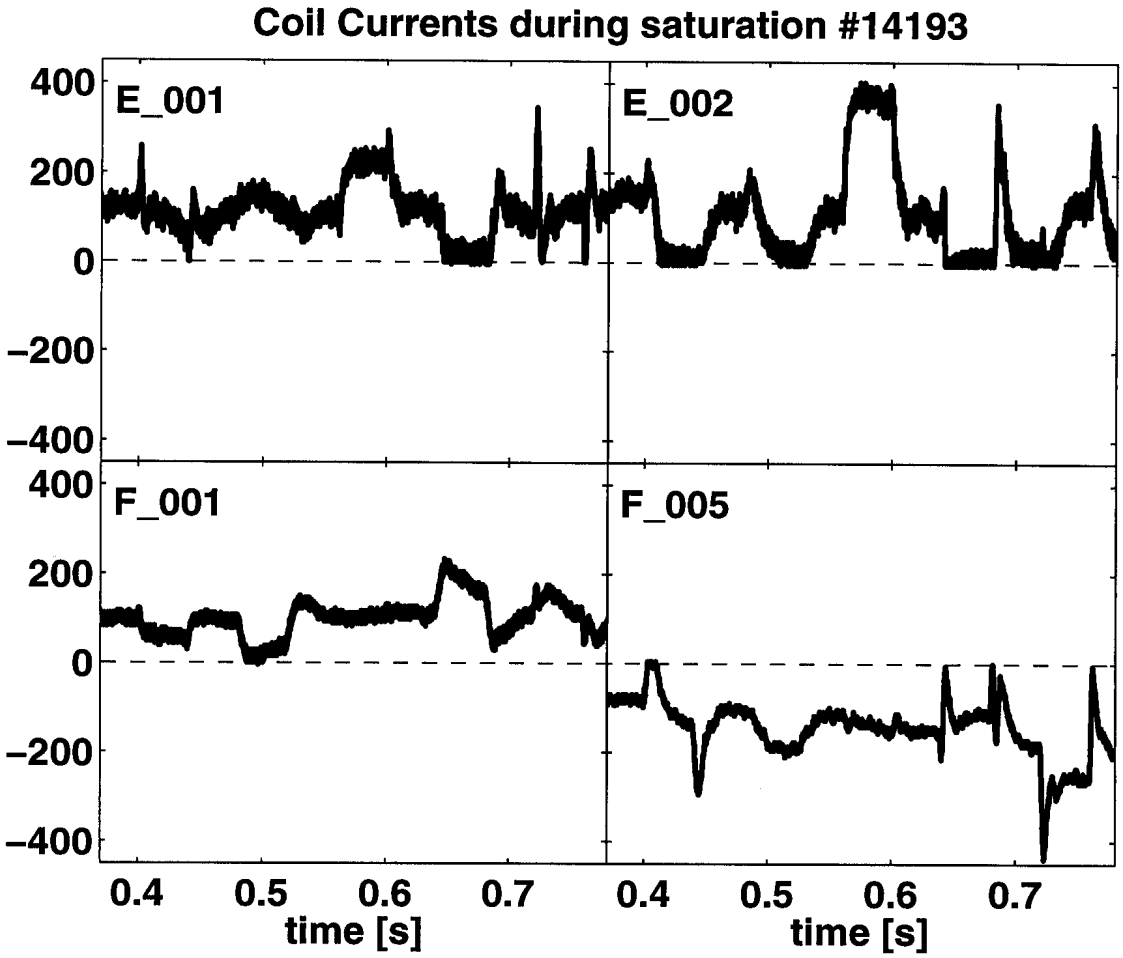

Figure 15. Evolution of some of the PF coil currents in ampères during the control response transients, illustrating the saturation at zero current.